STEM CELLS TRANSLATIONAL MEDICINE®

TISSUE-SPECIFIC PROGENITOR AND STEM CELLS

Epimuscular Fat in the Human Rotator Cuff Is a Novel Beige Depot

GRETCHEN A. MEYER,[a] MICHAEL C. GIBBONS,[a] EUGENE SATO,[a] JOHN G. LANE,[b] SAMUEL R. WARD,[b,c] ADAM J. ENGLER[a,d]

Key Words. Brown adipose tissue • Rotator cuff • Adipose stem cells • Skeletal muscle

Departments of [a]Bioengineering, [b]Orthopedic Surgery, and [c]Radiology, University of California, San Diego, La Jolla, California, USA; [d]Sanford Consortium for Regenerative Medicine, La Jolla, California, USA

Correspondence: Adam J. Engler, Ph.D., Department of Bioengineering, University of California, San Diego, 9500 Gilman Drive, MC 0695, La Jolla, California 92093, USA. Telephone: 858-246-0678; E-Mail: aengler@ucsd.edu

Received December 9, 2014; accepted for publication March 30, 2015; published Online First on May 21, 2015.

1066-5099/2015/$20.00/0

http://dx.doi.org/10.5966/sctm.2014-0287

ABSTRACT

Chronic rotator cuff (RC) tears are a common and debilitating injury, characterized by dramatic expansion of adipose tissue, muscle atrophy, and limited functional recovery. The role of adipose expansion in RC pathology is unknown; however, given the identified paracrine/endocrine regulation by other adipose depots, it likely affects tissue function outside its boundaries. Therefore, we characterized the epimuscular (EM) fat depot of the human rotator cuff, defined its response to RC tears, and evaluated its influence on myogenesis in vitro. EM fat biopsies exhibited morphological and functional features of human beige fat compared with patient-matched s.c. biopsies, which appeared whiter. The transcriptional profile of EM fat and isolated EM adipose-derived stem cells (ASCs) shifted as a function of the tear state; EM fat from intact cuffs had significantly elevated expression of the genes associated with uncoupled respiration, and the EM fat from torn cuffs had increased expression of beige-selective genes. EM ASC cocultures with human- and mouse-derived myogenic cells exhibited increased levels of myogenesis compared with s.c. cultures. Increased fusion and decreased proliferation of myogenic cells, rather than changes to the ASCs, were found to underlie this effect. Taken together, these data suggest that EM fat in the human rotator cuff is a novel beige adipose depot influenced by cuff state with therapeutic potential for promoting myogenesis in neighboring musculature. STEM CELLS TRANSLATIONAL MEDICINE *2015;4:764–774*

SIGNIFICANCE

Rotator cuff tears affect millions of people in the U.S.; however, current interventions are hindered by persistent muscle degeneration. This study identifies the therapeutic potential for muscle recovery in the epimuscular fat in the rotator cuff, previously considered a negative feature of the pathology, and finds that this fat is beige, rather than white. This is important for two reasons. First, the stem cells that were isolated from this beige fat are more myogenic than those from white fat, which have been the focus of stem cell-based therapies to date, suggesting epimuscular fat could be a better stem cell source to augment rotator cuff repair. Second, these beige stem cells promote myogenesis in neighboring cells in culture, suggesting the potential for this fat to be manipulated therapeutically to promote muscle recovery through secreted signals.

INTRODUCTION

Tears to one or more tendons of the rotator cuff (RC) are estimated to affect as much as 50% of the population older than 60 years [1], making RC disease one of the most common causes of musculoskeletal pain and loss of function in the U.S. Although acute surgical repairs have high rates of success, most presentations are chronic and degenerative, with repeat tear rates as high as 90%, depending on the tear size and chronicity [2, 3]. Fatty atrophy of the RC musculature is a defining feature of chronic tears with retraction and is highly negatively correlated with long-term repair success [4–6]. This process, typically discussed in terms of an "infiltration" or replacement of contractile material volume with fat, occurs in two places in the torn rotator cuff: inside the muscle (intramuscular) and outside the muscle (epimuscular). Although increases in both are associated with poor functional outcomes in RC tears, very little is known about these adipose depots. Even less is known about the process of fatty expansion in either compartment, which progenitor cells contribute to it, and its effect on muscle function after repair.

The muscles of the healthy rotator cuff are encapsulated by a thin layer of adipose tissue (epimuscular fat) similar to that found around the heart (epicardial fat) [7]. The function of this adipose depot is unknown, but it might play a protective role as a mechanical buffer between the

muscle and bone or be involved in the storage and release of fatty acids in response to the energy needs of the muscle, which has hypothesized for epicardial and perivascular adipose depots [7]. One thing is clear, however: this depot is not static or inert; it is dynamic and responds to environmental changes by mobilizing a progenitor population (e.g., an adipose-derived stem cell [ASC]) [8]. In cuffs with large chronic tears, the epimuscular fat depot expands to occupy as much as 75% of the healthy muscle volume [6].

Adipose tissue expansion can be viewed as a negative or positive change, depending on its anatomical location and type. The expansion of white subcutaneous or visceral fat is the defining feature of obesity and is associated with a host of health issues [9]. Numerous studies are attempting to promote the expansion of brown or beige/brite fat for its thermogenic properties [10, 11]. Classic brown fat has a distinct metabolic profile, and, in humans, it is primarily distinguished from white fat by its unique morphology and protein expression [12]. Beige or brite fat was recently identified in mice and humans and resembles classic brown fat; however, it shares a developmental origin with white fat [13, 14]. Because developmental lineage tracing is not possible in humans, debate continues about the "brownness" of human adipose depots [15, 16]. However, it is becoming increasingly clear that a number of human adipose depots have characteristics somewhere on the spectrum of beige/brite fat, including perivascular fat, epicardial fat, and the fat surrounding the kidneys, pancreas, and liver [17]. In addition to their more systemic roles in thermogenesis and whole-body energy metabolism, these depots are thought to contribute locally to the metabolic health and function of the tissues they surround [18, 19].

To date, the type of adipose depots in muscle, especially in the RC, and the potency of the progenitors in these depots remain unknown. Recent research has focused on anatomically distant white fat depots as a potential source of ASCs [20–22] for promoting rotator cuff healing. We hypothesized that epimuscular fat might represent a unique beige depot with therapeutic promise either as an autologous source of ASCs or as a modular source of paracrine myogenic signaling. Thus, we investigated the characteristics of epimuscular fat from both the intact and the torn human rotator cuff, to examine the phenotype of the depot and how it is affected by chronic RC disease. Additionally, because adipose tissue influences function outside its borders [23], we tested whether epimuscular ASCs participate in the regenerative processes in adjacent tissues (e.g., undergoing de novo myogenesis or signaling neighboring myogenic progenitors to undergo myogenesis). Our findings suggest that epimuscular fat might play a previously less appreciated role in muscle regeneration in the human rotator cuff.

Materials and Methods

Tissue Biopsies

Biopsies of adipose tissue surrounding rotator cuff musculature (epimuscular fat) and biopsies of subcutaneous adipose tissue were obtained from the shoulders of 30 patients undergoing arthroscopic rotator cuff surgery. The patients were classified into 2 groups by the operating surgeon: patients with an intact cuff (n = 11) and patients with a full or partial thickness tear to at least 1 tendon of the cuff (n = 19). Biopsies of the supraspinatus and infraspinatus muscles in the rotator cuff were obtained concurrently with the adipose biopsies, and isolated skeletal muscle progenitors were used for coculture experiments. The biopsies constituted approximately 10 mg of tissue. With the limited sample volume, the number of donors per group for each assay is listed in supplemental online Table 1. Lipoaspirate was obtained from an additional 6 patients undergoing liposuction for comparison with the other anatomical sources of adipose tissue. The institutional review board of the University of California, San Diego, Human Research Protection Program approved the present study (approval nos. 101878 and 090829 for liposuction and rotator cuff surgery, respectively), and all participants gave written informed consent to participate.

The patients recruited for the present study were a mixture of male and female subjects in all groups. No significant difference was present in the body mass index within the RC surgical patients (RC torn, 30.3 $\pm$ 1.7 kg/m^2; RC intact, 32.5 $\pm$ 1.6 kg/m^2). A significant difference was found in age between the 2 groups, however, with the torn RC group significantly older than the RC intact group (RC torn, 57 $\pm$ 3 years; RC intact, 46 $\pm$ 3 years). This difference is consistent with the reported increasing incidence of rotator cuff tears with age [1]. Tear severity also varied across the RC torn group, from a partial-thickness tear (n = 6) to a full-thickness tear without retraction (n = 8) to a full-thickness tear with retraction (n = 5).

Stem Cell and Progenitor Isolation

Adipose tissue biopsies and lipoaspirate were digested to isolate the ASC population, as previously described [24]. In brief, the biopsies were rinsed during transportation from the operating room in Dulbecco's modified Eagle's medium (DMEM; low glucose), transferred to a digestive solution composed of 0.3% collagenase type I, 60 U/μl dispase II, and 1% penicillin/streptomycin in low-glucose DMEM, minced with forceps, and allowed to incubate at 37°C for 30 minutes. The cells were then further dissociated by gentle pipetting, after which the samples were filtered through a 70-μm nylon mesh to remove debris. The suspension was then centrifuged, and the resulting pellet was resuspended in growth medium consisting of 10% fetal bovine serum and 1% penicillin/streptomycin in low-glucose DMEM and plated overnight at 37°C. Samples with adequate numbers of surviving cells were then culture expanded in growth medium, changing the medium every 2–3 days. Skeletal muscle progenitor (SMP) cells were isolated, as previously described [25]. In brief, muscle biopsies were digested in a solution containing collagenase type I and dispase II, mechanically dissociated, and filtered to yield a suspension of mononuclear cells. The cell suspensions were incubated with fluorophore-conjugated primary antibodies: neural cell adhesion molecule (NCAM) (BD Pharmingen, San Diego, CA, http://www.bdbiosciences.com), CD31 (eBioscience Inc., San Diego, CA, http://www.ebioscience.com), and CD45 (eBioscience). The NCAM+/CD31$-$/CD45$-$ population was then isolated using a FACSAria II (BD Biosystems) and expanded in culture to passage 3.

Cell Characterization Assays

The cell area and proliferation measures were acquired from low-passage cultures during culture expansion (i.e., fewer than 3 passages). The cell area was quantified from bright-field images by a blinded observer using the region of interest tracing tool in ImageJ (n = 10 cells per sample). The cell proliferation rates were calculated by serially tracking clonal expansion over the course of

5 days (n = 3–5 clones per sample). The long-term expansion capability was evaluated in a subset of cultures using a Click-iT EdU assay (Life Technologies, Carlsbad, CA, http://www.lifetechnologies.com) in accordance with the manufacturer's instructions. The percentage of proliferating cells in each culture at each passage was calculated as the ratio of EdU-positive nuclei to 4′,6-diamidino-2-phenylindole (DAPI)-positive nuclei using a custom detection algorithm designed in MATLAB.

Cell Differentiation Conditions

For the adipogenic differentiation assays, the ASC cultures were grown to confluence in growth medium, after which they were switched to an adipogenic induction medium consisting of 0.1 μM dexamethasone, 10 μM indomethacin, 0.5 mM 3-isobutyl-1-methylxanthine, 10 μg/ml insulin, and 1% penicillin/streptomycin in low-glucose DMEM. The cultures were maintained in adipogenic induction medium for 14 days, changing the medium every 2–3 days. For isoproterenol-activated assays, 10 μM (final) isoproterenol was added to the culture medium, and the cells were incubated for an additional 12 hours. For mechanical induction of myogenesis, the cells were seeded at a low density (5,000 cells per well) on polyacrylamide matrix-coated, 25-mm diameter coverslips. Matrices of muscle-mimicking stiffness (e.g., 10 kPa [a unit of stiffness]) were fabricated and functionalized with fibronectin protein, as previously described [26]. The cells were then cultured in growth medium for the indicated time period. The cells were simultaneously cultured on uncoated glass coverslips as a negative control. To induce terminal differentiation and fusion, the ASCs were cocultured with myogenic progenitor cells of either mouse (C2C12) or human (SMP) origin. The ASCs were initially plated and expanded to 75% confluence. Next, C2C12s or Vybrant CFDA (Life Technologies)-labeled SMPs were added to the culture in a 1:20 or 1:5 ratio, respectively. The cocultures were cultured in a myogenic induction medium consisting of 5% horse serum, 10 μg/ml insulin, and 1% penicillin/streptomycin in low-glucose DMEM for 7 days.

Histology and Immunostaining Assays

For histological analysis, the adipose biopsies were fixed in 0.5% paraformaldehyde for 2 hours, submerged in sucrose overnight at 4°C, embedded in optimal cutting temperature compound, and flash frozen in liquid nitrogen-cooled isopentane. Next, 16-μm-thick sections were cut from the midsection of the sample using a Leica Cryocut 3000 (Leica, Heerbrugg, Switzerland, http://www.leica.com) at −30°C. Adipose tissue cryosections and ASC cultures were fixed with 3.7% formaldehyde for 15 minutes, permeabilized with 1% Triton X-100 for 10 minutes, and blocked with a solution of 20% goat serum and 0.3% Triton X-100 in phosphate-buffered saline (PBS) for 1 hour. The sections were then incubated with the following primary antibodies at the listed dilutions for 1 hour: uncoupling protein 1 (UCP1) (1:250; U6382; Sigma-Aldrich, St. Louis, MO, http://www.sigmaaldrich.com), MyoD (1:50;M-318; Santa Cruz Biotechnology Inc., Santa Cruz, CA, http://www.scbt.com), Myf5 (1:50; C-20; Santa Cruz Biotechnology), myosin heavy chain (1:30; MF20; Developmental Studies Hybridoma Bank, University of Iowa, Iowa City, IA), and human lamin A (1:250; ab108595; Abcam, Cambridge, U.K., http://www.abcam.com). The samples were then rinsed with PBS, incubated with a fluorophore-conjugated secondary antibody (1:400; Life Technologies) for 20 minutes, rinsed again, and counterstained with Hoechst 33342 (1:1000; Life Technologies) for 2 minutes. The samples were imaged using a CARVII confocal microscope (BD Biosciences, San Diego, CA, http://www.bdbiosciences.com) using a CoolSNAP HQ camera (Photometrics, Tucson, AZ, http://www.photometrics.com) controlled by Metamorph 7.6 software (Molecular Devices, Sunnyvale, CA, http://www.moleculardevices.com).

Quantification of Myf5 immunofluorescence was automated by a custom-designed MATLAB algorithm, which integrated the Myf5 signal over DAPI-positive pixels. The cells were considered positive if their nuclear Myf5 intensity was more than 2 SDs above the mean from the control cultures. Myogenic indexes were quantified using a semiautomated algorithm designed in MATLAB. The number of lamin A-positive or -negative nuclei within myosin heavy chain-positive myotubes were counted and divided by the total number of lamin A-positive or -negative nuclei in the field, respectively.

Quantitative Polymerase Chain Reaction

To obtain sufficient RNA for quantitative polymerase chain reaction analysis, the patient biopsies were frozen and then pooled by tear state (2–3 patients per pool). RNA was extracted from the pooled biopsies and individual ASC cultures using a TRIzol-based assay (Life Technologies), and cDNA was created using Superscript III reverse transcriptase (Life Technologies), as previously described [27]. Transcript copies were detected using a SYBR Green PCR master mix (Applied Biosystems, Foster City, CA, http://www.appliedbiosystems.com) combined with 800 nm of each primer. The primer sets are listed in supplemental online Table 2. Reactions were run in duplicate with the following reaction profile: 2 minutes at 50°C and 10 minutes at 95°C, followed by 40 cycles of 15 seconds at 95°C and 1 minute at 60°C. The expression values were calculated using a standard curve generated by a fibronectin plasmid and then normalized to *glyceraldehyde-3-phosphate dehydrogenase* expression. Hierarchical clustering was performed using Cluster and TreeView software (Eisen Lab, Howard Hughes Medical Institute at University of California, Berkeley, and the Lawrence Berkeley National Laboratory, Berkeley, CA, http://www.eisenlab.org). Expression of each gene was centered to its mean and normalized, and the gene set was subjected to centroid linkage clustering with a centered correlation.

Flow Cytometry

Flow cytometry was performed on suspended cells against two positive markers for lipoaspirate-derived ASCs (CD90 [1:100; eBioscience] and CD105 [1:100; eBioscience]) and three negative markers (CD45 [1:100; eBioscience], CD31 [1:100; eBioscience], and NCAM [1:100; BD Pharmingen]). An unstained portion of the sample was used to set the positive-negative gates. Data acquisition was performed using an LSR Fortessa (BD Biosystems), and analysis was performed using FlowJo data analysis software (FlowJo, LLC, Ashland, OR, http://www.flowjo.com). Expression was considered positive for any cell with a fluorescent intensity greater than 99% of the unstained population.

Bioenergetic Assays

To measure cellular respiration, the cells were seeded into uncoated 96-well plates (XF96; 12,000 cells per well; Seahorse Bioscience, Billerica, MA, http://www.seahorsebio.com), grown to

confluence, and exposed to adipogenic induction medium for 14 days. On the day of the experiment, the wells were washed with assay medium consisting of 2 mM GlutaMAX (Life Technologies), 10 mM pyruvate, 10 mM glucose, and 10 mM HEPES in XF Medium (Seahorse Bioscience) and allowed to equilibrate for 1 hour. The oxygen consumption rate (OCR) was measured using an XF Analyzer (Seahorse Bioscience) at intervals of 6 minutes after mixing with the following compounds: oligomycin (1 μM final), carbonyl cyanide-*p*-trifluoromethoxyphenylhydrazone (2 μM final), and rotenone and antimycin A (2 μM final). The samples were run in sextuplicate and measures repeated in triplicate. After the measurements, the plates were fixed and stained with Hoechst 33342, and the cell density was computed using a custom detection algorithm designed in MATLAB. The OCR was then internally normalized to the cell density and externally normalized to the subcutaneous average basal respiration. Wells with negative or abnormal respiration values were discarded.

Statistical Analysis

The data were analyzed using one-way analysis of variance (ANOVA) with Bonferroni post hoc multiple testing correction, a Kruskal-Wallis test with a Dunn's multiple comparison test, or a two-tailed Student's *t* test, as applicable. Gene expression data were analyzed as a function of isoproterenol treatment with two-way ANOVA against group and treatment. Differences were considered significant at $p < .05$. All results are presented as the mean $\pm$ SEM.

Results

Epimuscular Adipose Biopsies Resemble Human Beige Fat

Striking differences in adipocyte size were identified between the epimuscular (EM) and s.c. adipose biopsies. The adipocytes from the EM biopsies were approximately one-fifth as large as those from the s.c. biopsies (Fig. 1A), a characteristic also noted in beige adipose tissue [28, 29]. Similarly, histological sections of the EM biopsies were characterized by small, predominately unilocular, adipocytes (Fig. 1B, open arrowheads), although small numbers of multilocular adipocytes were identified (Fig. 1B, closed arrowheads). These sections exhibited brighter staining for UCP1, a characteristic of beige fat, compared with the s.c. sections (Fig. 1B). To further investigate these differences quantitatively, the biopsies were pooled and assayed for expression of typical brown and beige markers (e.g., *UCP1* and *CD137*, respectively). The EM tissue showed a trend toward higher expression of UCP1 compared with the s.c. tissue, especially EM tissue from intact rotator cuffs (Fig. 1C). Biopsies of EM tissue from torn rotator cuffs showed a trend toward higher expression of *CD137* compared with either EM tissue from intact rotator cuffs or s.c. tissue (Fig. 1D).

Transcriptional Profile of Epimuscular ASCs Is a Function of Rotator Cuff Tear State

Because of the biopsy size limitations inherent to arthroscopic surgery, we turned to an in vitro model of isolated and culture expanded ASCs to further probe gene expression. ASCs have been shown to reflect parent adipose tissue gene expression [16]. Isolated EM ASCs were also significantly smaller than the s.c. ASCs but rapidly divided in culture and maintained their proliferative

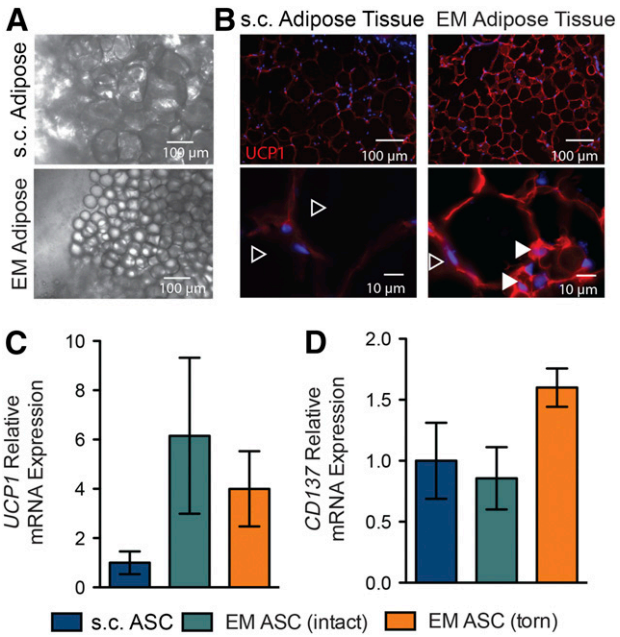

Figure 1. Morphology and expression profiles of EM adipose biopsies resemble human brown/beige fat. **(A):** Low-magnification light microscope images of freshly isolated biopsies of EM and s.c. adipose tissues. **(B):** Histological staining of adipose tissue sections for the brown fat marker *UCP1*. Closed versus open arrowheads indicate multilocular versus unilocular adipocytes. Quantitative polymerase chain reaction expression of the brown fat gene *UCP1* **(C)** and the beige gene *CD137* **(D)** relative to patient-matched s.c. biopsies for the indicated EM adipose biopsies as a function of rotator cuff tear state. Abbreviations: ASC, adipose-derived stem cell; EM, epimuscular.

ability (supplemental online Fig. 1) and surface marker expression (supplemental online Fig. 2) over several passages. In the undifferentiated state, ASCs from EM adipose tissue expressed significantly higher levels of the brown/beige fat transcriptional regulator *PRDM16*, independent of the rotator cuff state, compared with the s.c. ASCs. This suggests that even in the undifferentiated state, these cells have an identity tied to their tissue of origin (Fig. 2A). However, once cultures were induced to differentiate into adipocytes, distinct tear state differences in gene expression were apparent. Differentiated ASC cultures evaluated against a panel of 12 genes composed of characteristically white (*HOXC8*), brown (*UCP1*, *LHX8*, *CITED1*, *CIDEA*, *PGC1A*, *FBXO31*, and *ZIC1*), and beige (*TMEM26*, *CD137*, *TBX1*, and *HOXC9*) genes indicated that, although EM ASCs had significantly lower expression of the white fat gene *HOXC8* than did the s.c. ASCs, regardless of tear state (Fig. 2B), EM ASCs from intact cuffs exhibited significant induction of the characteristically brown genes *UCP1*, *LHX8*, *CITED1*, and *CIDEA* compared with s.c. ASCs. However, no significant induction was observed for EM ASCs from torn rotator cuffs (Fig. 2C). In contrast, EM ASCs from torn cuffs exhibited significantly increased expression of the beige gene *CD137* (Fig. 2D). EM ASCs from both intact and torn cuffs has significantly decreased expression of the characteristically brown fat gene *ZIC1*, mirroring the gene expression pattern in epicardial fat [29]. The expression was decoupled from the body mass index (BMI) and age (supplemental online Fig. 3). Given the large variation in gene expression in the characterized adult human depots [16], we also compared the expression in patient-matched EM

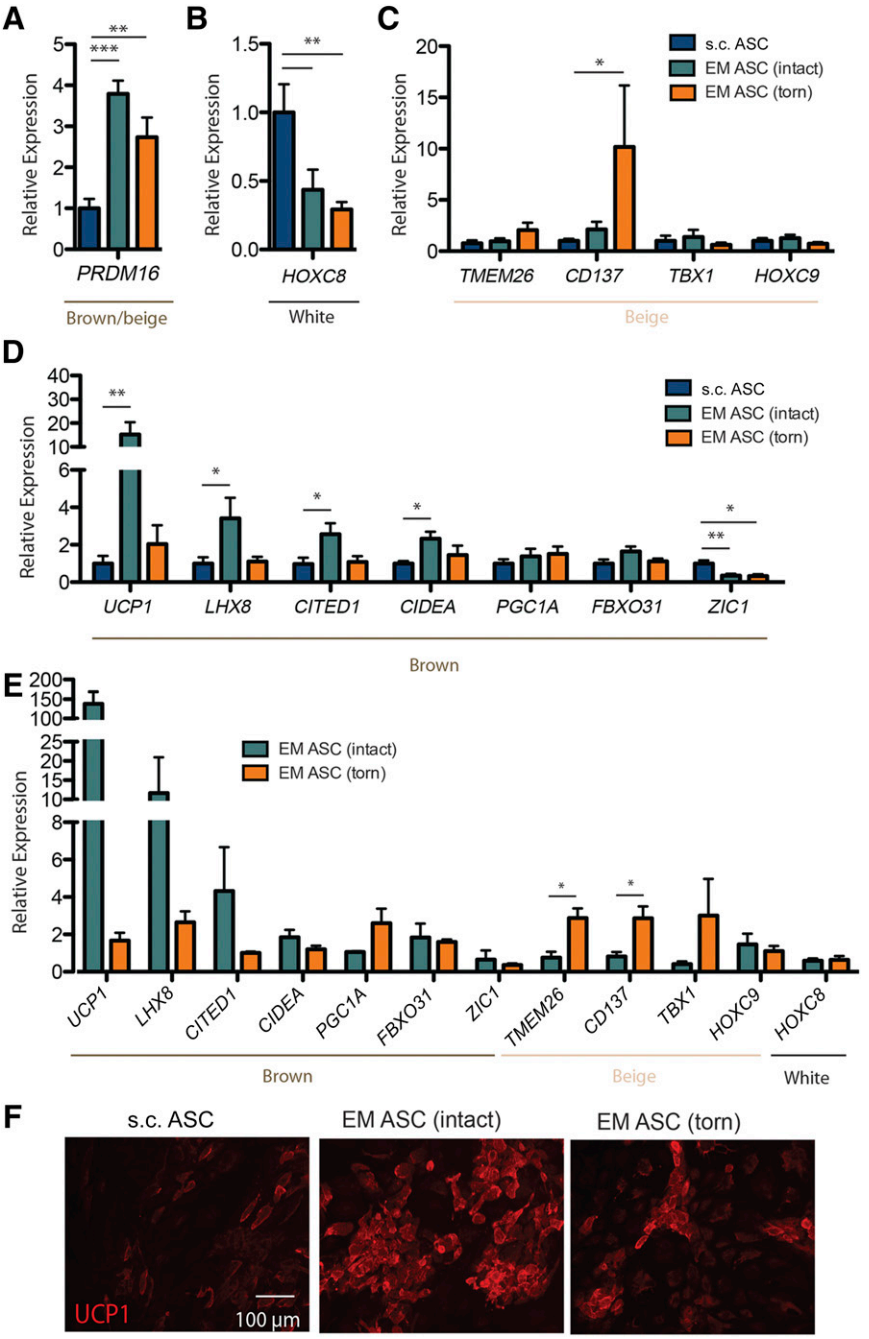

Figure 2. Expression profiles of EM ASCs resemble human brown/beige fat. **(A):** Undifferentiated ASCs of the indicated origin are plotted for their expression of the brown fat transcriptional regulator *PRDM16*. Expression of white **(B)**, beige **(C)**, and brown **(D)** genes is plotted for differentiated ASCs. **(E):** Gene expression for those markers in **B–D** was also evaluated and internally normalized (EM/s.c.) for patient-matched samples. **(F):** Immunofluorescent images of UCP1 protein qualitatively reflect gene expression data with brighter signal in EM ASC (intact) cultures. *, $p < .05$; **, $p < .01$; ***, $p < .001$. Abbreviations: ASCs, adipose-derived stem cells; EM, epimuscular; UCP1, uncoupling protein 1.

and s.c. cultures. When expression data were internally normalized to s.c., *UCP1* expression in the EM ASC-intact group was more than 100-fold higher than that in the patient-matched s.c. ASCs. Furthermore, the relative expression of the beige genes *TMEM26* and *CD137* was significantly higher in the EM ASCs from torn cuffs than that in those from intact cuffs (Fig. 2E). Given that gene expression data do not always correlate with protein abundance, the UCP1 protein in ASCs was assessed via immunostaining. EM ASC cultures from intact cuffs had significantly brighter UCP1 staining than did either EM ASCs from torn cuffs or s.c. ASCs (Fig. 2F).

Isoproterenol treatment has been classically shown to increase expression of brown and beige genes in nonwhite adipose tissue [14]. To further assess the ASC state, isoproterenol-treated ASCs were re-evaluated for their expression of a panel of adipose genes, subjected to hierarchical clustering, and found to cluster into three groups, identifiable by heat map (Fig. 3). The samples clustered into groups with low expression of beige and brown

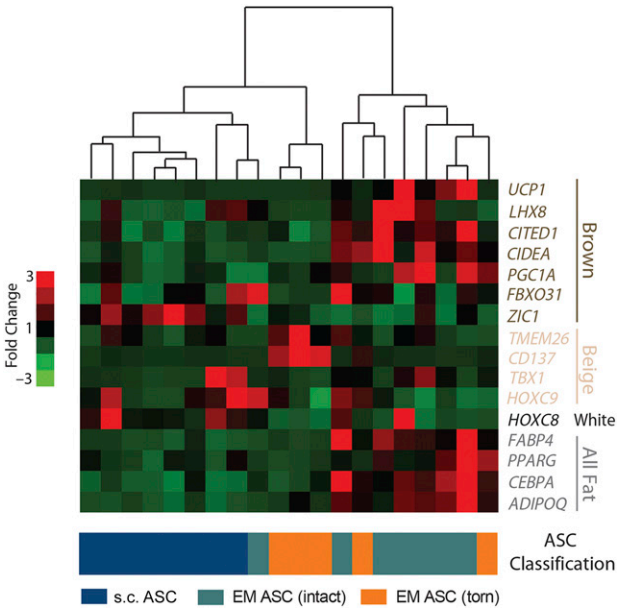

Figure 3. Activated EM ASCs cluster according to tear state across adipose genes. Expression of a panel of brown, beige, white, and all fat genes in isoproterenol-activated ASC cultures is shown in a heat map, with red colors indicating high expression and green colors indicating low expression. Hierarchical clustering (centroid linkage) is shown above the heat map, and the sample classification is shown below. Abbreviations: ASC, adipose-derived stem cell; EM, epimuscular.

genes but high expression of *HOXC8* (left), groups with high expression of beige genes (middle), and groups with high expression of brown genes (right), corresponding to samples of predominately s.c. tissue, predominately EM torn cuffs, and predominately EM intact cuffs, respectively. These data agree with the data from untreated cells (Fig. 2) and further substantiate that rotator cuff tears induce a change in the epimuscular adipose transcriptional profile.

To determine whether the gene expression changes corresponded to functional differences, mitochondrial respiration was measured in a subset of differentiated ASCs. The basal normalized OCR was slightly elevated in the EM samples relative to the s.c. samples, suggesting an increased mitochondrial density in these samples (Fig. 4A, 4B). The OCR after oligomycin treatment [line (i) in Fig. 4A], which measures only uncoupled respiration, was significantly elevated in the EM samples compared with the s.c. samples (Fig. 4C). This difference is on the order of what has been measured previously in unstimulated human cervical ASCs compared with s.c. ASCs [30, 31]. No difference was found in uncoupled respiration between the torn and intact cuffs, despite differences in *UCP1* expression between these groups. However, a significant positive correlation was observed between the expression of *UCP1*, and its transcriptional regulator *CIDEA*, and measured uncoupled respiration (r^2 = .183 and r^2 = .475, respectively), suggesting that the lack of difference in functional respiration might arise from patient-to-patient variability in this subset of samples. Together, these differences at least establish a functional difference between s.c. and EM ASCs.

Early Myogenesis and Fusion in EM ASCs Depends on Tear State

Visceral ASCs have a previously reported myogenic capacity [32], and, together with the anatomical location of EM adipose, there was compelling evidence to assess their myogenic ability. Extracellular matrix stiffness cues are more effective than chemical cues at inducing visceral ASC myogenesis [27]; thus, EM ASCs from both intact and torn cuffs were cultured for 7 days on substrates that mimicked the stiffness of muscle (e.g., 10 kPa) [33]. Compared with s.c. ASCs, EM ASCs had significantly more cells expressing myogenic transcription factors Myf5 and MyoD in response to myogenic stiffness (Fig. 5A). The percentage of Myf5-positive cells was significantly higher in the EM ASC cultures than in the s.c. ASC cultures, regardless of the tear state, and was higher in the intact cuff sources than in the torn cuff sources (Fig. 5B). When gene expression was evaluated over the 7-day culture, increases in *MYOD1* expression were highest for EM ASCs, specifically those from intact rotator cuffs (Fig. 5C).

To determine whether this difference is maintained beyond early myogenesis, we investigated the capacity of EM ASCs to terminally fuse into myotubes in a coculture assay with SMPs isolated from the same patient cohort. In a myogenic induction medium, CFDA-labeled ASCs (Fig. 6A, left column) were able to heterotypically fuse with SMPs to form myosin heavy chain (MHC)-positive myotubes (Fig. 6A, center column) regardless of source. Overlap of the green and red signals indicate the myotubes with ASC contributions (Fig. 6A, right column, arrowheads). Expression of early- (*MYOD*), mid- (*MEF2C*), and late (*MHC*)-stage myogenic genes revealed a significant MyoD expression increase in cocultures with EM ASCs from intact cuffs and a significant MHC expression increase in cocultures with EM ASCs from torn cuffs compared with s.c. ASCs (Fig. 6B). However to distinguish between direct (i.e., fusion) and indirect (i.e., signaling) contributions of ASC populations to myogenesis in coculture, an interspecies coculture system was used. Coculture of human-derived ASCs with murine-derived C2C12 myoblasts allowed for clear delineation between nuclei arising from human (Fig. 7A, red) and mouse (Fig. 7A, blue) sources and allowed us to identify myotube fusion (Fig. 7A, green). Consistent with human coculture, coculture of EM ASCs with murine-derived C2C12 cells resulted in higher overall expression of MyoD and MHC. However, increased expression was restricted to the C2C12 population, and levels were unchanged between the ASC populations (Fig. 7B). This difference was reflected in the fusion indexes, in which the percentage of the ASC population terminally differentiating into myotubes was not different between the sources (Fig. 7C), but the percentage of the C2C12 population in myotubes was higher if they were cultured with EM ASCs than if they were cultured with s.c. ASCs (Fig. 7D). Despite cell density differences between cultures, ASC proliferation was consistent between sources, yielding no differences in cell density at the end of the culture period (Fig. 7E). However, the C2C12 density was significantly higher in coculture with s.c. ASCs than with EM ASCs, reflecting increased proliferation during the culture period (Fig. 7F). These data indicate that in the presence of committed myogenic cells, EM ASCs can act through paracrine or cell-cell signals to enhance fusion but that s.c. adipose promotes expansion of these myogenic cells.

Discussion

Classically, brown adipose tissue is thought to arise from a lineage that is distinct from white fat and more closely related to muscle [34–36]. Recent studies identifying a distinct intermediate adipose type in rodents, termed "beige" or "brite," have implicated

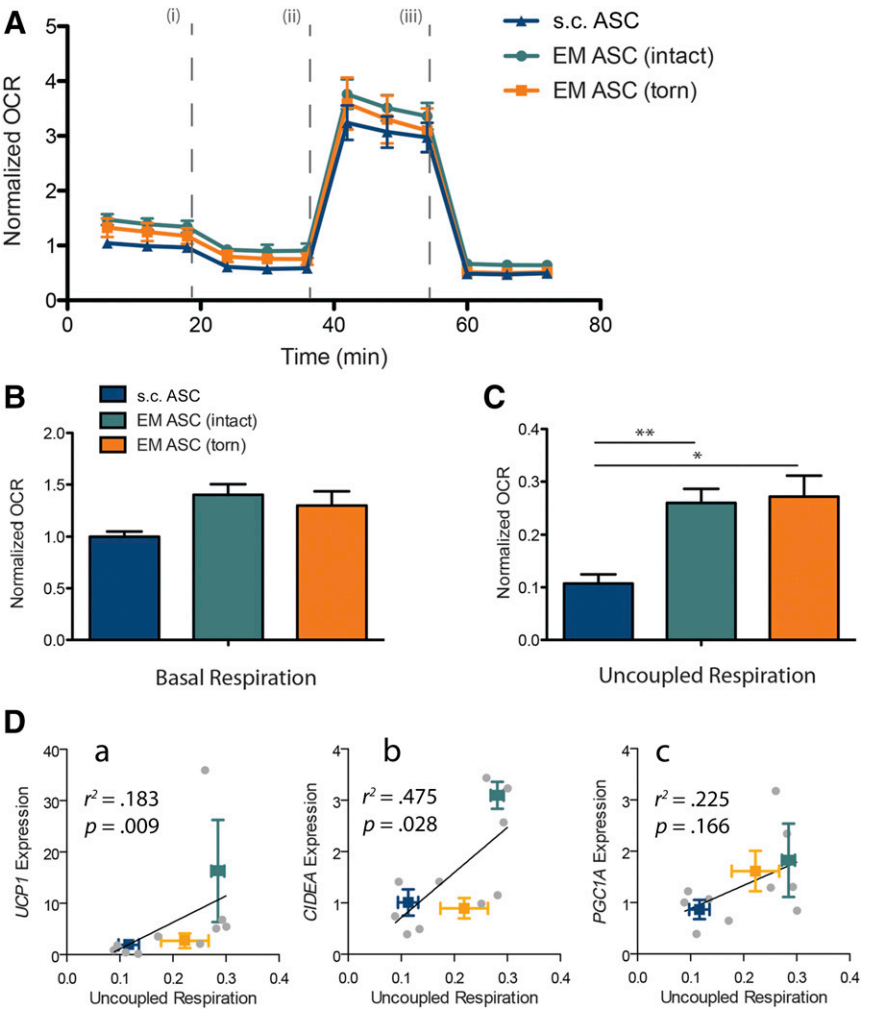

Figure 4. EM ASCs have higher uncoupled respiration compared with s.c. ASCs. **(A):** Plot of the relative OCRs of ASC cultures from s.c. and EM sources. Raw OCR values are first normalized by cellular density and then to s.c. average basal respiration. Drug injection sequence is noted by roman numerals: oligomycin (i), carbonyl cyanide-*p*-trifluoromethoxyphenylhydrazone (ii), and rotenone and antimycin A (iii). **(B):** Plot of basal respiration in EM cultures compared with s.c. cultures. **(C):** Plot of uncoupled respiration. **(D):** Regression of uncoupling-linked genes *UCP1* (a), *CIDEA* (b), and *PGC1A* (c) against uncoupled respiration. ∗, $p < .05$; ∗∗, $p < .01$. Abbreviations: ASCs, adipose-derived stem cells; EM, epimuscular; OCR, oxygen consumption rate.

a "browning" of classically white depots in response to stimulation rather than transdifferentiation in brown fat [13, 14]. In humans, this issue is complicated by the identification of novel adipose depots, not previously identified as white, exhibiting beige characteristics in homeostasis [7, 16, 29]. Whether these tissues represent transdifferentiated white depots, specialized brown depots, or a totally unique subset of adipose tissues is still a topic of intense debate [11, 37]. However, regardless of their origin, beige depots in humans represent an intriguing and, thus far, poorly understood tissue type.

Origin and Type of Epimuscular Fat

Our data suggest that EM fat from the human rotator cuff is a novel beige depot, exhibiting 2- to 10-fold higher *UCP1* expression compared with s.c. tissue but lower than that in brown fat depots [16]. Combined with the morphological features typical of beige fat (i.e., small and predominately unilocular adipocytes [14, 29]), these data are suggestive of a beige rather than a brown depot. However, gene expression analysis in fresh biopsies was complicated by the exceedingly small sample size and mRNA amount that could be isolated even from pooled biopsies of 3–4 patients. Furthermore, pooling patients prevented data regression against patient demographics or normalization of expression within a patient. Because *UCP1* expression has been shown to vary more than 1,000 fold between patients in a given depot [16] and is likely influenced by factors such as age and body mass index, additional investigation was performed on unpooled populations of ASCs. These cultured and differentiated cells have been shown to maintain gene expression profiles of the tissue from which they were derived [16], despite differences that could arise given their time in culture.

Tear State Influences the Transcriptional Profile of Epimuscular Fat

Epimuscular ASCs also expressed increased levels of classically brown and beige genes but interestingly seemed to differentiate in expression as a function of the cuff tear state. Cells isolated from torn cuffs expressed higher levels of the beige genes

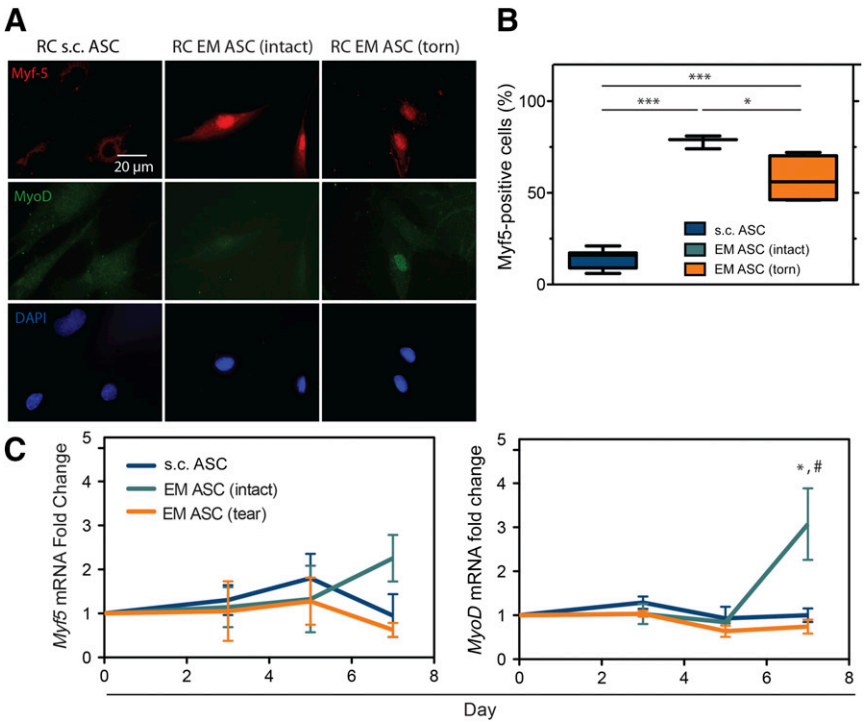

Figure 5. EM ASCs exhibit increased stiffness-directed early myogenesis. **(A):** Immunofluorescent images of ASCs cultured on hydrogels of muscle-like stiffness and stained for two transcriptional markers of myogenesis, Myf5 (top) and MyoD (middle). **(B):** Quantification of Myf5 immunofluorescence in these cultures. A positive signal was determined relative to an undifferentiated control for each culture. ∗, $p < .05$; ∗∗, $p < .01$; ∗∗∗, $p < .001$. **(C):** Gene expression data for *Myf5* and *MyoD* at day 7 for the indicated sources and tear states. ∗, $p < .05$ compared with RC s.c. ASCs; #, $p < .05$ compared with RC EM ASCs (torn). Abbreviations: ASCs, adipose-derived stem cells; DAPI, 4′,6-diamidino-2-phenylindole; EM, epimuscular; RC, rotator cuff.

TMEM26 and *CD137* and lower levels of the brown genes *UCP1*, *LHX8*, *CITED1*, and *CIDEA* compared with intact cuffs. However, it is important to note that the "classically brown" genes we examined are not unique to brown fat but are also expressed to a lesser degree in beige fat, depending on the level of uncoupled respiration, frequently referred to as a degree of "browning." The degree to which identified human beige fat depots express classically brown and beige fat genes also varies as a function of anatomical location, which could explain the low expression of *TBX1* (thought to be a preferential marker for subcutaneous beige depots only) and *ZIC1* (thought to be absent from all beige depots) in EM ASCs [38]. Taken together with the minor elevation in functional uncoupled respiration compared with s.c. tissue, these data suggest that EM ASCs from intact cuffs have a decreased potential for browning compared with those from intact cuffs, rather than a transition from a brown phenotype to a beige phenotype.

The idea that beige adipose depots can alter their characteristics in response to external stimuli is supported by studies that have demonstrated increased thermogenic features after treatment with β-agonists [39] or chronic exposure to peroxisome proliferation-activated receptor γ agonists [13]. However, our ability to define the factors responsible for this shift here was complicated by the factors intrinsic to the patient population being studied. For example, rotator cuff tear incidence increases with age [1, 40], a feature reflected by the older population in the torn versus intact cuff group. *UCP1* expression has been noted to decrease as a function of age in both brown and beige depots [41, 42]. However, no significant correlation was found between *UCP1* expression and either age or BMI in our data (supplemental online Fig. 3). Furthermore, no difference was found in age between the intact and torn groups in the subset of patient-matched data; however, significant differences were still noted as a function of tear state (Fig. 2E). Another confounding factor was that the patients classified as having an intact cuff did not necessarily have a healthy shoulder. They were undergoing surgery to address pain or limited range of motion in the glenohumeral joint, meaning they represent a heterogeneous population with varying degrees of tissue damage, inflammation, and fibrosis. Future mechanistic studies delving into the regulators of gene expression in epimuscular adipose tissue will likely need to turn to in vitro or animal models to avoid these issues.

Signaling Within the Rotator Cuff

Recent studies have provoked renewed interest in adipose tissue depots for their local and systemic effects as an endocrine organ [23, 43]. These effects are not unique to white fat. A recent study by Rahman et al. pointed to the endocrine/paracrine effect that murine beige fat has on remodeling in the skeleton [19]. Our findings demonstrating the unique effects that human epimuscular ASCs exert on myogenesis in coculture further suggest that beige fat might influence cells outside its borders. Especially in chronic rotator cuff tears, in which the epimuscular depot expands dramatically concurrent with large maladaptations in the musculature, resulting in a blurring of the muscle-fat boundary, it is likely that substantial cross-talk is present between these tissues. Furthermore, during surgical repair, the retracted muscle is placed under substantial traction, perhaps initiating signals for

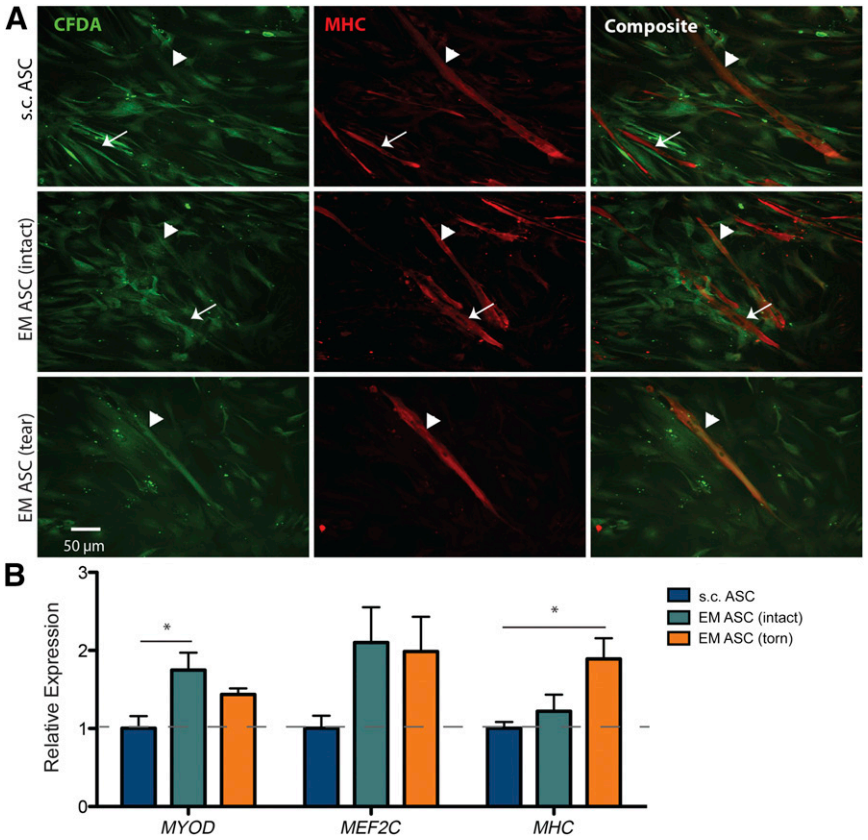

Figure 6. EM and s.c. ASCs are capable of fusion with skeletal muscle progenitor (SMP) cells derived from rotator cuff muscles. **(A):** Images of CFDA-labeled ASCs (green, left panel) fused with rotator cuff-derived SMPs in differentiated cocultures from the indicated patient cohorts. Arrowheads indicate CFDA-positive myotubes and arrows, CFDA-negative myotubes. **(B):** Expression of early (*MYOD*), mid (*MEF2C*), and late (*MHC*) stage myogenic genes as a function of ASC source, normalized to s.c. ASC average expression. $*$, $p < .05$. Abbreviations: ASCs, adipose-derived stem cells; EM, epimuscular.

activation, proliferation, and differentiation of muscle progenitor cells. Our data suggest that signals from the epimuscular fat might inhibit proliferation and promote differentiation of these cells. This effect is most pronounced in cocultures with EM ASCs from torn cuffs, because these cultures express the highest levels of the late differentiation marker myosin heavy chain and the highest myogenic index. Although differentiation is a key step in the response cycle of muscle progenitor cells to injury, early differentiation at the expense of proliferation has been shown to be highly detrimental to the muscle's ability to recover from injury [44, 45].

Therapeutic Implications

Taken together, these data suggest the intriguing possibility that the large stores of fat in the torn rotator cuff, previously considered a negative feature of the disease, present a novel therapeutic opportunity to enhance muscle regeneration after surgical repair. On one hand, the increased multipotency of EM ASCs and their unique effects on myogenic cells in culture suggest that they might be a more promising stem cell source than the previously evaluated s.c. ASCs for improving cuff healing [20–22]. On the other hand, the beige characteristics of EM fat suggest that they could be "browned," which is associated with the secretion of various growth factors upstream of the muscle repair and hypertrophy pathways [19, 46, 47]. Despite these data, many steps exist between two-dimensional coculture and human rotator cuff physiology that should be addressed. The present study has demonstrated the potential for this fat in promoting muscle regeneration in vitro, the next studies will take these cells into an in vivo animal model to prove their therapeutic potential and evaluate the mechanisms by which epimuscular fat might promote myogenesis after injury. Such data will substantially improve our understanding of the muscle and fat pathophysiology in the human rotator cuff.

Conclusion

Epimuscular adipose tissue in the human rotator cuff is a novel depot, unique from the subcutaneous fat of the shoulder. The gene expression profile, morphology, and mitochondrial respiration of biopsies and cultured adipose-derived stem cells resembles newly identified human beige fat. Furthermore, the gene expression profile of cells derived from intact cuffs differs from that of torn cuffs, suggesting that the environment of the torn rotator cuff could be signaling adaptation in this tissue. Cells derived from epimuscular fat promote differentiation and inhibit proliferation of myogenic progenitor cells in coculture, suggesting epimuscular fat could have a unique signaling effect on the muscles of the human rotator cuff.

Acknowledgments

We thank Drs. Meagan McCarthy and Morgan Silldorff for assistance with sample acquisition; Dr. Anastasia Kralli and Enrique

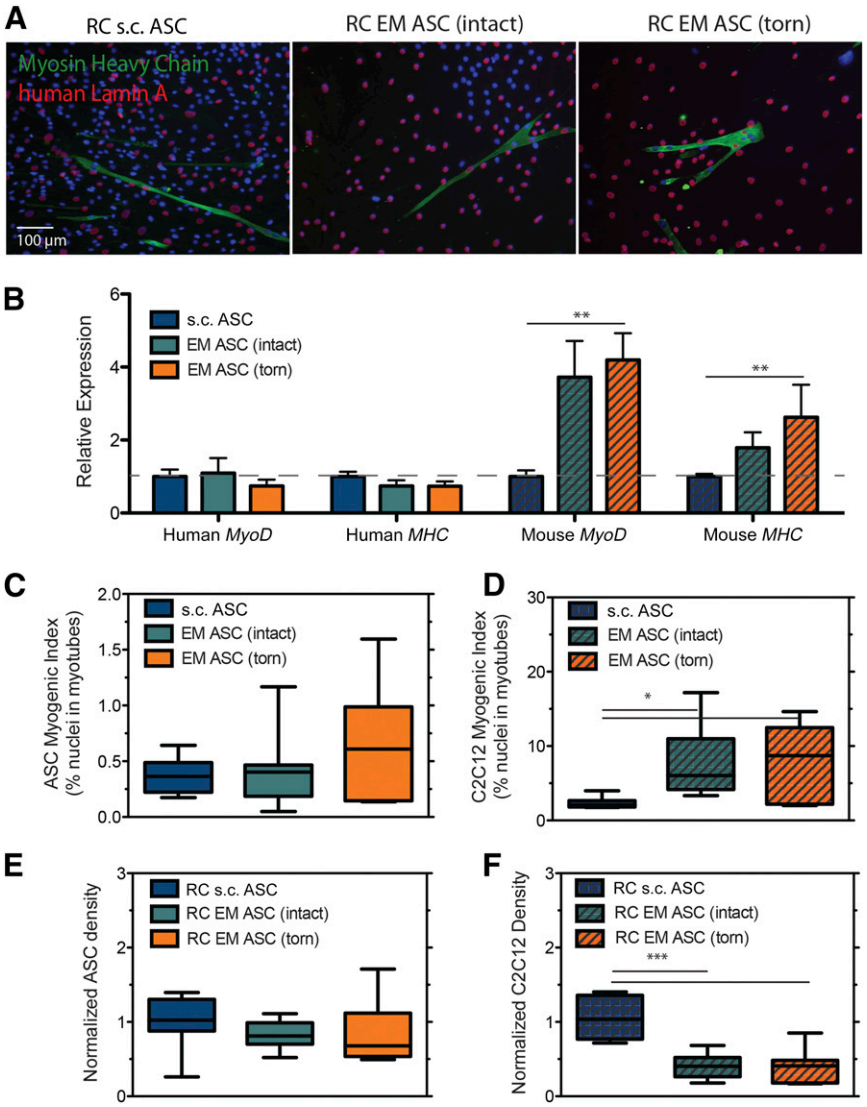

Figure 7. Epimuscular ASCs affect C2C12 proliferation and fusion in coculture. **(A):** Immunofluorescent images of cross-species (human ASC and murine C2C12) coculture. ASC nuclei are identified using a human-specific antibody to lamin A (red), and myotubes are identified by myosin heavy chain (*MHC*; green). Myotubes were identified containing both human and mouse nuclei in all cultures. No myotubes were identified containing only human nuclei. **(B):** Quantification of species-specific isoform expression of *MyoD* and *MHC*. Gene expression values were normalized to s.c. ASC average expression. **(C):** Plot of the ASC myogenic index, defined as the percentage of total lamin A-positive nuclei in *MHC*-positive structures. **(D):** Plot of the C2C12 myogenic index, defined as the percentage of total lamin A-negative nuclei in *MHC*-positive structures. At the end of the culture period, the density of ASCs **(E)** and the density of C2C12 cells **(F)** was assessed from cocultures. Culture densities were normalized to the s.c. ASC average. $*$, $p < .05$; $**$, $p < .01$; $***$, $p < .001$.

Saez, Andrea Galmozzi, and Christina Godio for help with bioenergetics analysis; and Dr. Simon Schenk for helpful discussions. We acknowledge the National Institutes of Health (Grant F32AR063588 to G.A.M., Grant R01HD073180 to S.R.W., Grant AR061303 to S.R.W. and A.J.E., and Grant DP02OD006460 to A.J.E.) and the Muscular Dystrophy Association (Grant 241665 to A.J.E.) for funding support. G.A.M. is currently affiliated with the Program in Physical Therapy, Washington University School of Medicine, St. Louis, MO.

Author Contributions

G.A.M.: conception and design, provision of study material or patients, performance of experiments, data analysis and interpretation, manuscript writing, financial support; M.C.G.: provision of study material or patients, performance of experiments, data analysis and interpretation; E.S. and J.G.L.: provision of study material or patients; S.R.W.: conception and design, data analysis and interpretation, manuscript writing, financial support; A.J.E.: conception and design, data analysis and interpretation, manuscript writing, financial support, final approval of manuscript.

Disclosure of Potential Conflicts of Interest

J.G.L. is a compensated consultant with Vericel (Carticel) and has compensated stock options in Parcus Medica, COAST Surgery Center. The other authors indicated no potential conflicts of interest.

REFERENCES

1 Sher JS, Uribe JW, Posada A et al. Abnormal findings on magnetic resonance images of asymptomatic shoulders. J Bone Joint Surg Am 1995;77:10–15.

2 Galatz LM, Ball CM, Teefey SA et al. The outcome and repair integrity of completely arthroscopically repaired large and massive rotator cuff tears. J Bone Joint Surg Am 2004;86-A: 219–224.

3 Bishop J, Klepps S, Lo IK et al. Cuff integrity after arthroscopic versus open rotator cuff repair: A prospective study. J Shoulder Elbow Surg 2006;15:290–299.

4 Gerber C, Schneeberger AG, Hoppeler H et al. Correlation of atrophy and fatty infiltration on strength and integrity of rotator cuff repairs: A study in thirteen patients. J Shoulder Elbow Surg 2007;16:691–696.

5 Gladstone JN, Bishop JY, Lo IKY et al. Fatty infiltration and atrophy of the rotator cuff do not improve after rotator cuff repair and correlate with poor functional outcome. Am J Sports Med 2007;35:719–728.

6 Shen P-H, Lien S-B, Shen H-C et al. Long-term functional outcomes after repair of rotator cuff tears correlated with atrophy of the supraspinatus muscles on magnetic resonance images. J Shoulder Elbow Surg 2008;17(suppl):1S–7S.

7 Iozzo P. Myocardial, perivascular, and epicardial fat. Diabetes Care 2011;34(suppl 2): S371–S379.

8 Gimble JM, Katz AJ, Bunnell BA. Adipose-derived stem cells for regenerative medicine. Circ Res 2007;100:1249–1260.

9 Flier JS. Obesity wars: Molecular progress confronts an expanding epidemic. Cell 2004; 116:337–350.

10 Wu J, Cohen P, Spiegelman BM. Adaptive thermogenesis in adipocytes: Is beige the new brown? Genes Dev 2013;27:234–250.

11 Nedergaard J, Cannon B. How brown is brown fat? It depends where you look. Nat Med 2013;19:540–541.

12 Virtanen KA, Lidell ME, Orava J et al. Functional brown adipose tissue in healthy adults. N Engl J Med 2009;360:1518–1525.

13 Petrovic N, Walden TB, Shabalina IG et al. Chronic peroxisome proliferator-activated receptor gamma (PPARgamma) activation of epididymally derived white adipocyte cultures reveals a population of thermogenically competent, UCP1-containing adipocytes molecularly distinct from classic brown adipocytes. J Biol Chem 2010;285:7153–7164.

14 Wu J, Boström P, Sparks LM et al. Beige adipocytes are a distinct type of thermogenic fat cell in mouse and human. Cell 2012;150: 366–376.

15 Sharp LZ, Shinoda K, Ohno H et al. Human BAT possesses molecular signatures that resemble beige/brite cells. PLoS ONE 2012;7:e49452.

16 Jespersen NZ, Larsen TJ, Peijs L et al. A classical brown adipose tissue mRNA signature partly overlaps with brite in the supraclavicular region of adult humans. Cell Metab 2013;17: 798–805.

17 Sacks H, Symonds ME. Anatomical locations of human brown adipose tissue: Functional relevance and implications in obesity and type 2 diabetes. Diabetes 2013;62:1783–1790.

18 Rabkin SW. Epicardial fat: Properties, function and relationship to obesity. Obes Rev 2007;8:253–261.

19 Rahman S, Lu Y, Czernik PJ et al. Inducible brown adipose tissue, or beige fat, is anabolic for the skeleton. Endocrinology 2013;154:2687–2701.

20 Valencia Mora M, Antuña Antuña S, García Arranz M et al. Application of adipose tissue-derived stem cells in a rat rotator cuff repair model. Injury 2014;45(suppl 4):S22–S27.

21 Barco R, Encinas C, Valencia M et al. Use of adipose-derived stem cells in an experimental rotator cuff fracture animal model. Rev Esp Cir Ortop Traumatol 2015;59:3–8.

22 Oh JH, Chung SW, Kim SH et al. 2013 Neer Award: Effect of the adipose-derived stem cell for the improvement of fatty degeneration and rotator cuff healing in rabbit model. J Shoulder Elbow Surg 2014;23:445–455.

23 Ahima RS, Flier JS. Adipose tissue as an endocrine organ. Trends Endocrinol Metab 2000;11:327–332.

24 Choi YS, Dusting GJ, Stubbs S et al. Differentiation of human adipose-derived stem cells into beating cardiomyocytes. J Cell Mol Med 2010;14:878–889.

25 Meyer GA, Farris AL, Sato E et al. Muscle progenitor cell regenerative capacity in the torn rotator cuff. J Orthop Res 2015;33:421–429.

26 Tse JR, Engler AJ. Preparation of hydrogel substrates with tunable mechanical properties. Curr Protoc Cell Biol 2010;10:10.16.1–10.16.16.

27 Choi YS, Vincent LG, Lee AR et al. Mechanical derivation of functional myotubes from adipose-derived stem cells. Biomaterials 2012;33:2482–2491.

28 Cypess AM, White AP, Vernochet C et al. Anatomical localization, gene expression profiling and functional characterization of adult human neck brown fat. Nat Med 2013;19:635–639.

29 Sacks HS, Fain JN, Bahouth SW et al. Adult epicardial fat exhibits beige features. J Clin Endocrinol Metab 2013;98:E1448–E1455.

30 Lee P, Werner CD, Kebebew E et al. Functional thermogenic beige adipogenesis is inducible in human neck fat. Int J Obes (Lond) 2014; 38:170–176.

31 Lee P, Linderman JD, Smith S et al. Irisin and FGF21 are cold-induced endocrine activators of brown fat function in humans. Cell Metab 2014;19:302–309.

32 Di Rocco G, Iachininoto MG, Tritarelli A et al. Myogenic potential of adipose-tissue-derived cells. J Cell Sci 2006;119:2945–2952.

33 Engler AJ, Griffin MA, Sen S et al. Myotubes differentiate optimally on substrates with tissue-like stiffness: Pathological implications for soft or stiff microenvironments. J Cell Biol 2004;166:877–887.

34 Timmons JA, Wennmalm K, Larsson O et al. Myogenic gene expression signature establishes that brown and white adipocytes originate from distinct cell lineages. Proc Natl Acad Sci USA 2007;104:4401–4406.

35 Atit R, Sgaier SK, Mohamed OA et al. Beta-catenin activation is necessary and sufficient to specify the dorsal dermal fate in the mouse. Dev Biol 2006;296:164–176.

36 Seale P, Bjork B, Yang W et al. PRDM16 controls a brown fat/skeletal muscle switch. Nature 2008;454:961–967.

37 Giralt M, Villarroya F. White, brown, beige/brite: Different adipose cells for different functions? Endocrinology 2013;154:2992–3000.

38 Lidell ME, Betz MJ, Dahlqvist Leinhard O et al. Evidence for two types of brown adipose tissue in humans. Nat Med 2013;19: 631–634.

39 Himms-Hagen J, Melnyk A, Zingaretti MC et al. Multilocular fat cells in WAT of CL-316243-treated rats derive directly from white adipocytes. Am J Physiol Cell Physiol 2000;279: C670–C681.

40 Tempelhof S, Rupp S, Seil R. Age-related prevalence of rotator cuff tears in asymptomatic shoulders. J Shoulder Elbow Surg 1999;8: 296–299.

41 Heaton JM. The distribution of brown adipose tissue in the human. J Anat 1972;112: 35–39.

42 Sacks HS, Fain JN, Holman B et al. Uncoupling protein-1 and related messenger ribonucleic acids in human epicardial and other adipose tissues: Epicardial fat functioning as brown fat. J Clin Endocrinol Metab 2009;94: 3611–3615.

43 Scherer PE. Adipose tissue: From lipid storage compartment to endocrine organ. Diabetes 2006;55:1537–1545.

44 Palacios D, Mozzetta C, Consalvi S et al. TNF/p38α/polycomb signaling to Pax7 locus in satellite cells links inflammation to the epigenetic control of muscle regeneration. Cell Stem Cell 2010;7:455–469.

45 Tierney MT, Aydogdu T, Sala D et al. STAT3 signaling controls satellite cell expansion and skeletal muscle repair. Nat Med 2014;20: 1182–1186.

46 Yamashita H, Sato N, Kizaki T et al. Norepinephrine stimulates the expression of fibroblast growth factor 2 in rat brown adipocyte primary culture. Cell Growth Differ 1995;6: 1457–1462.

47 Hansson HA, Nilsson A, Isgaard J et al. Immunohistochemical localization of insulin-like growth factor I in the adult rat. Histochemistry 1988;89:403–410.

See www.StemCellsTM.com for supporting information available online.